ACS Biomaterials SCIENCE & ENGINEERING

pubs.acs.org/journal/abseba

Letter

Optimization of Culture Media and Cell Ratios for 3D *In Vitro* Skeletal Muscle Tissues with Endothelial Cells

John SK Yuen Jr., Brigid M Barrick, Hailey DiCindio, Jaymie A Pietropinto, and David L Kaplan*

Cite This: *ACS Biomater. Sci. Eng.* 2023, 9, 4558−4566

Read Online

ACCESS | Metrics & More | Article Recommendations | Supporting Information

ABSTRACT: A major challenge of engineering larger macroscale tissues *in vitro* is the limited diffusion of nutrients and oxygen to the interior. For skeletal muscle, this limitation results in millimeter scale outcomes to avoid necrosis. One method to address this constraint may be to vascularize *in vitro*-grown muscle tissue, to support nutrient (culture media) flow into the interior of the structure. In this exploratory study, we examine culture conditions that enable myogenic development and endothelial cell survival within tissue engineered 3D muscles. Myoblasts (C2C12s), endothelial cells (HUVECs), and endothelial support cells (C3H 10T1/2s) were seeded into Matrigel-fibrin hydrogels and cast into 3D printed frames to form 3D *in vitro* skeletal muscle tissues. Our preliminary results suggest that the simultaneous optimization of culture media formulation and cell concentrations is necessary for 3D cultured muscles to exhibit robust myosin heavy chain expression and GFP expression from GFP-transfected endothelial cells. The ability to form differentiated 3D muscles containing endothelial cells is a key step toward achieving vascularized 3D muscle tissues, which have potential use as tissue for implantation in a medical setting, as well as for future foods such as cultivated meats.

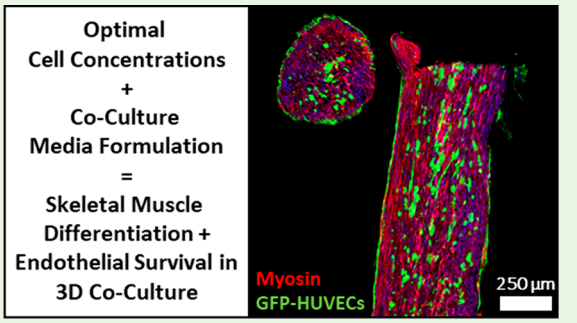

KEYWORDS: *vascularization, endothelialization, skeletal muscle, cultivated meat, cultured meat, coculture, 3D culture*

INTRODUCTION

3D culture approaches to produce skeletal muscle tissues would be advantageous for regenerative medicine goals as well as towards producing cultivated meat. *In vitro* grown muscle tissue with the aligned muscle fiber structure and organization found within *in vivo* muscle provides for robust tissues for a range of needs, from restoration of damaged muscle tissue *in vivo* (volumetric muscle loss) to future foods as whole muscle (structured) cell-culturedmeats.[1] In medical tissue engineering and regenerative medicine, implanting 3D cultured skeletal muscle with aligned arrays of myofibers offers a method to address injuries to the tissue where normal regenerative processes are absent.[2,3]

The major challenge to engineering macroscale muscle tissues is the limited diffusion of nutrients and O_2 to cells in the interior of *in vitro* constructs.[4] As a result, efforts to create *in vitro* muscles have been typically limited to the millimeter scale.[5−9] A potential technique for producing larger *in vitro* muscles may be to vascularize them with endothelial cells. In 3D culture, endothelial cells form capillary-like blood vessels that resemble *in vivo* microvasculature.[10−12] This vascular network may permit the growth of larger tissues by allowing culture media to reach cells in the interior of macroscale constructs, or through muscle-endothelial cell signaling. Indeed, *in vitro*-grown muscles cocultured with endothelial cells showed improved tissue performance after implantation.[13−15]

In this study, we aimed to generate myosin-expressing, 3D *in vitro* muscle tissues capable of supporting cocultured endothelial cells.[15] To achieve this, media formulations were selected for their potential in supporting the simultaneous culture of muscle and endothelial cells, then tested on cocultures of these cell types in a 3D culture system designed for the cultivation of *in vitro* muscle as small bundles on the micrometer (thickness) to millimeter (length) scale. Ratios of muscle to endothelial cells were also investigated to search for parameters that best supported endothelial cell survival and muscle differentiation.

MATERIALS AND METHODS

Cell Culture. GFP-HUVECs were purchased from Angio-Proteomie (cAP-0001GFP), then cultured in Endothelial Cell Growth Medium 2 (ECGM2, cAP-02; Angio-Proteomie) at 37 °C and 5% CO_2 (≤passage 5). Murine myoblasts (C2C12s) were

Received: March 19, 2023
Accepted: June 12, 2023
Published: June 16, 2023

Table 1. Culture Media Formulations Used to Culture *In Vitro* Muscle

Culture media	Formulation
2HS-EBM	EBM (5.55 mM glucose) with 2% horse serum, 1X insulin-transferrin-selenium-ethanolamine (ITSE-Animal Free, 777ITS032; InVitria, Junction City, KS, USA), 0.05% AlbuMAX I (11020021; ThermoFisher), 0.75 mg/mL 6ACA, and PenStrep
Muscle Coculture Media (MCCM)	EBM with 1X ECGM-MV2 SupplementMix (C-39226, Promocell), 9.5 ng/mL VEGF (100−44; Shenandoah Biotechnology Inc., Warminster, PA, USA), 1X ITSE, 0.05% AlbuMAX I, 0.75 mg/mL 6ACA, 10 nM DEX, 30 ng/mL IGF-1, 250 nM sphingosine-1-phosphate (S1P, 62570; Cayman Chemicals), and PenStrep; ECGM-MV2 gives this formulation a final 5% FBS
MCCM (-S1P)	MCCM excluding 250 nM S1P
10FBS-I	EBM with 10% FBS, 10 μg/mL insulin (I0516; Sigma-Aldrich), 100 ng/mL IGF-1, 0.75 mg/mL 6ACA, PenStrep
MCCM2	A 1:1 mix of MCCM and 10FBS-I media

obtained from the American Type Culture Collection (ATCC), used between passages X+4 and X+8 (X denoting an unknown # of passages), and cultured in 10FBS-DMEM: Dulbecco's modified eagle medium (DMEM, 10569044; ThermoFisher, Waltham, MA, USA), 10% fetal bovine serum (FBS, A31606-01, ThermoFisher), 1% antibiotic/antimycotic (Anti/Anti, 15240062; ThermoFisher) at 37 °C and 5% CO_2. Murine C3H 10T1/2s were purchased from the ATCC (CCL-226 and CRL-3268 for unmodified and mRuby expressing cells respectively) and expanded in 10FBS-DMEM, with occasional addition of 2 μg/mL blasticidin (sc-495389; Santa Cruz Biotechnology, Dallas, TX, USA) to maintain mRuby expression. Both types of 10T1/2 cell lines were ≤ passage 30. Cryopreservation of all cells was achieved by mixing media with DMSO (D2438; Sigma-Aldrich) at a ratio of 9:1 (medium:DMSO), after which the cells were frozen in isopropanol-based freezing containers (5100-0001; ThermoFisher) overnight at −80 °C before long term liquid nitrogen storage.

2D Differentiation of Skeletal Muscle. To differentiate the myoblasts, C2C12s were seeded at 40,000 cells/cm^2 in 48 well plates and cultured to confluency in 10FBS-DMEM. After reaching confluency, cells were switched for 7 days to either: (1) Endothelial Basal Medium (EBM; Promocell) supplemented with 2% horse serum (16050130; ThermoFisher), Penicillin-Streptomycin (100 U/mL and 100 μg/mL, respectively, PenStrep, 15140122; ThermoFisher), and 0.75 mg/mL 6 aminocaproic acid (6ACA, A7824, Sigma-Aldrich), or (2) Muscle Coculture Media (MCCM, Table 1).

Muscle differentiation was quantified via the fusion index, which is defined as the proportion of nuclei that reside within myosin heavy chain (MHC) staining myotubes. The fusion index was calculated in ImageJ by first using MHC fluorescence as a mask to exclude nonmyotube nuclei and then counting the number of DAPI stained nuclei using the "Find Maxima" function. This number was then compared to the total number of DAPI stained nuclei.[16]

3D Cultures. 3D muscles were cultured in 3D printed miniature-wells (2 mm × 2 mm × 10 mm, using a biocompatible resin: Surgical Guide resin; Formlabs, Somerville, MA, USA). Mini-wells were adhered onto the surface of noncell culture-treated 6 well plate wells using medical device epoxy (MED-301; Epoxy Technology Inc., Billerica, MA, USA). Mini-wells contained small posts (0.4 mm ⌀) 1 mm from each end of the wells. The posts limited hydrogel compaction and generated tension in the growing tissues to stimulate muscle differentiation (Figure S1). On the day of 3D culture, the mini-wells were incubated with 5% Pluronic F127 (poloxamer 407 - polypropylene glycol and polyethylene glycol copolymer, dissolved in water, P2443; Sigma-Aldrich) for 30 min to inhibit tissue adherence to the mini-wells. After incubation, the Pluronic F127 was vacuum aspirated out, and mini-wells were allowed to dry.

3D muscle cultures were generated by first thawing Matrigel (8.5 mg/mL, 356234; Corning Inc.) overnight at 4 °C. Then 50 U/mL bovine thrombin (T4648; Sigma-Aldrich, dissolved in water) was thawed on ice. Next, 20 mg/mL bovine fibrinogen (341573; Sigma-Aldrich, gently dissolved in 0.9% NaCl saline) was thawed in a 37 °C water bath and then kept at room temperature until right before mixing cells and hydrogel components, which took place on ice. Fibrinogen was kept away from the ice whenever possible to avoid precipitation during extended incubation on ice or at 4 °C (data not shown).

Next, the required cells (C2C12s ± GFP-HUVECs and C3H-10T1/2s) were detached from their culture flasks using trypsin-EDTA 0.25% (25200056; ThermoFisher), Accumax (AM105; Innovative Cell Technologies), and TrypLE (12604013; ThermoFisher), respectively, then resuspended to 10 million cells/mL in EBM. These suspensions were then mixed with each other to achieve desired cell ratios in the final hydrogel, which were based on preliminary experiments (data not shown) and examples in the literature.[17−19] On ice, Matrigel and fibrinogen were added to the cell suspensions, mixed, then the combined solution was added to mini-wells containing a small amount of thrombin (0.95 μL, for a total of 38 μL cell + hydrogel solution per mini-well), and then mixed via micropipette 4 times while filling all areas of the well with liquid (no air pockets). The gels were then left to polymerize upside down at 37 °C, 5% CO_2 for 30 min. Final Matrigel-fibrin (MF) hydrogel concentrations were 1.25 mg/mL Matrigel, 1.25 mg/mL fibrinogen, 1.25 U/mL thrombin, 2−5 million C2C12s/mL, 1−2 million HUVECs/mL, and 250−500k 10T1/2s/mL. (For monocultures only containing C2C12s, the cell concentration was 10 million C2C12s/mL) After 30 min, culture media was added to the cell-laden hydrogels. The various culture media used to culture the *in vitro* muscles are outlined in (Table 1). After 1−2 days, parts of the 3D skeletal muscles that were still adhered to the walls of the mini-wells were detached by scraping against the walls using 22−24 gauge needles. All muscle constructs were cultured in 3D for a total of 14 days.

Fluorescent and Immunofluorescent Staining of In Vitro Muscle Samples. At the end of the tissue culture (7 or 14 days of differentiation), samples were fixed in 4% paraformaldehyde (PFA, J19943K2; ThermoFisher) for 10 min (2D) or 1 h (3D), then washed 3 times with DPBS (10 min incubations per wash for 3D tissues). Samples were stored at 4 °C if not immediately stained.

For 2D samples, samples were rinsed with a blocking/permeabilization (B/P) buffer [DPBS with 0.1% Tween 20 (P2287; Sigma), 5% goat serum (16210−064; ThermoFisher), 0.3 M Glycine (161−0718; Bio-Rad, Hercules, CA, USA), and 0.02% sodium azide (S2002; Sigma)], and then incubated in more B/P buffer for 45−60 min. After incubation, samples were incubated overnight at 4 °C with primary antibodies diluted in B/P buffer (2.5 μg/mL, anti-MHC, MF20, Developmental Studies Hybridoma Bank, Iowa City, IA, USA). The next day, samples were rinsed with DPBS (2 min incubation) and incubated with B/P buffer containing secondary antibodies (1:500, Goat Anti-Mouse Alexa Fluor Plus 594, A32742; ThermoFisher), 1:1000 Phalloidin-iFluor 488 (ab176753; Abcam, Cambridge, United Kingdom), 1 μg/mL DAPI (4′,6-diamidino-2-phenylindole, 62248; ThermoFisher) for 2 h at RT, protected from light. Secondary antibodies and other compounds were then rinsed from the samples using DPBS twice (2 min incubations/wash). Lastly, samples were mounted in Vectashield Vibrance (H-1700; Vector Laboratories, Burlingame, CA, USA) and imaged via confocal microscopy (SP8; Leica, Wetzlar, Germany).

3D samples underwent a similar staining procedure but were first cryoprotected and flash frozen. First, 3D muscle bundles were placed in 20% sucrose (S0389, Sigma-Aldrich) overnight. Then, samples

https://doi.org/10.1021/acsbiomaterials.3c00358
ACS Biomater. Sci. Eng. 2023, 9, 4558−4566

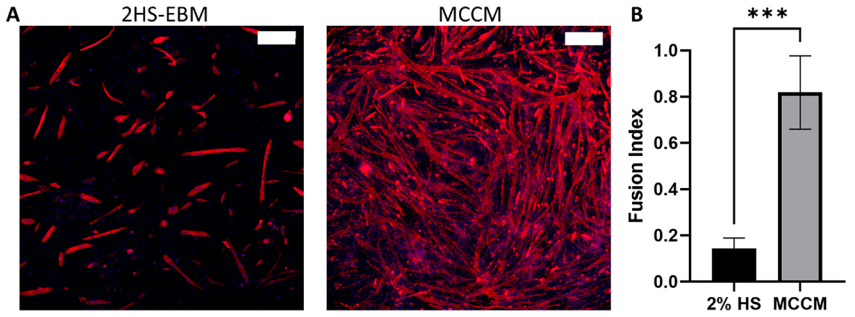

Figure 1. Myoblasts cultured in 2D with a 2% horse serum-based differentiation media, or a coculture medium formulation. (A) Myosin heavy chain (red) stain of C2C12 myoblasts differentiated for 7 days in 2HS-EBM or MCCM. Scale bars represent 200 μm. (B) Fusion index (% nuclei residing in MHC+ myofibers) measurements to quantify muscle differentiation in A. n = 3 for MCCM and 4 for 2HS-EBM. (***) represents $p \leq 0.001$.

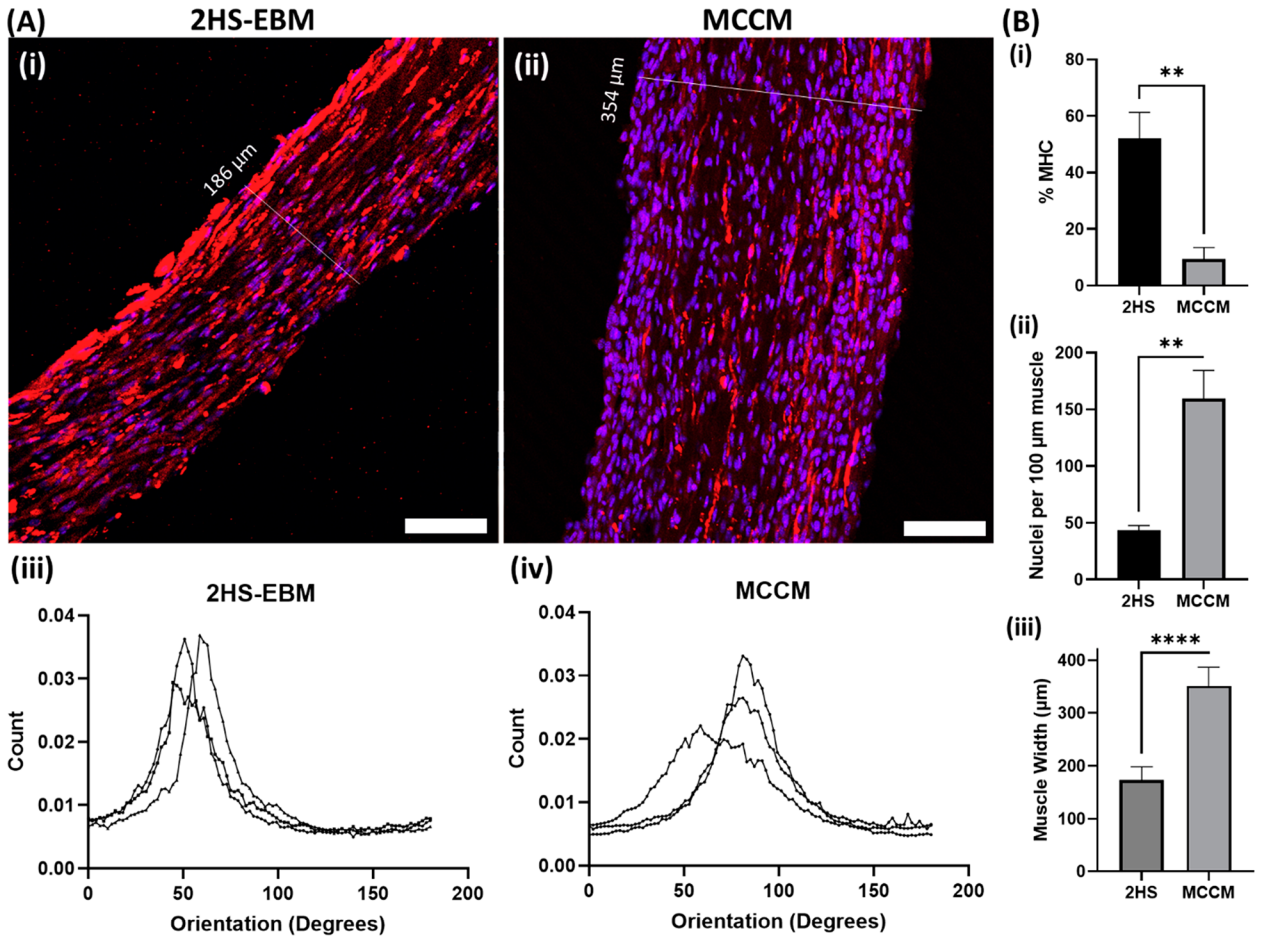

Figure 2. Muscle cells cultured in 3D with a 2% horse serum-based differentiation medium, or a muscle-endothelial coculture medium. (A) (i, ii) Cryosectioned, *in vitro*-grown 3D muscles stained for nuclei (blue) and MHC (red). C2C12s (10 million cells/mL) in MF gels were grown in either 2HS-EBM or MCCM for 14 days. Scale bar represents 100 μm. (iii, iv) Myotube alignment data for each sample group. Count refers to the proportion of structures aligned toward a particular orientation. (B) (i) Measures of *in vitro* muscle construct width for A. n = 3 with 10 measurements per sample. (****) is $p \leq 0.0001$. (ii) Area fraction of muscle construct cryosections from (A) that are MHC+. (**) is $p \leq 0.01$. (iii) Number of nuclei counted per 100 μm length of *in vitro* muscle cryosections from A. N = 3 for all data in this figure.

were moved to 50% sucrose/50% optimal cutting temperature compound (OCT, 23−730−571; Fisher Scientific, Waltham, MA, USA) for 1 h, and then 30% sucrose/70% OCT for another hour, and then 100% OCT for 30 min. Subsequently, samples were placed in plastic embedding molds (2.4 cm × 2.4 cm × 0.5 cm) with fresh OCT and flash frozen in liquid nitrogen, taking care to not have the sample contact the nitrogen. Frozen samples were then cryosectioned (CM1950; Leica) onto glass slides (Superfrost Gold; 15−188−48, Fisher Scientific), stained like 2D samples, and sealed with a glass coverslip. Cryosections were cut 30 μm thick and the middle (thickest portion) of the *in vitro* tissues were selected (visually) for sectioning. For certain experiments, staining jars were used during some staining steps (in place of pipetting liquids directly onto the slides) in order to reduce tissue delamination from the glass slides.

From the cryosections, % MHC^+ and GFP^+ were calculated by measuring the % area of the section where MHC or GFP stain was present. Muscle width was determined by manually making 10 measurements (per cryosection) perpendicular to the long axis of the

https://doi.org/10.1021/acsbiomaterials.3c00358
ACS Biomater. Sci. Eng. 2023, 9, 4558−4566

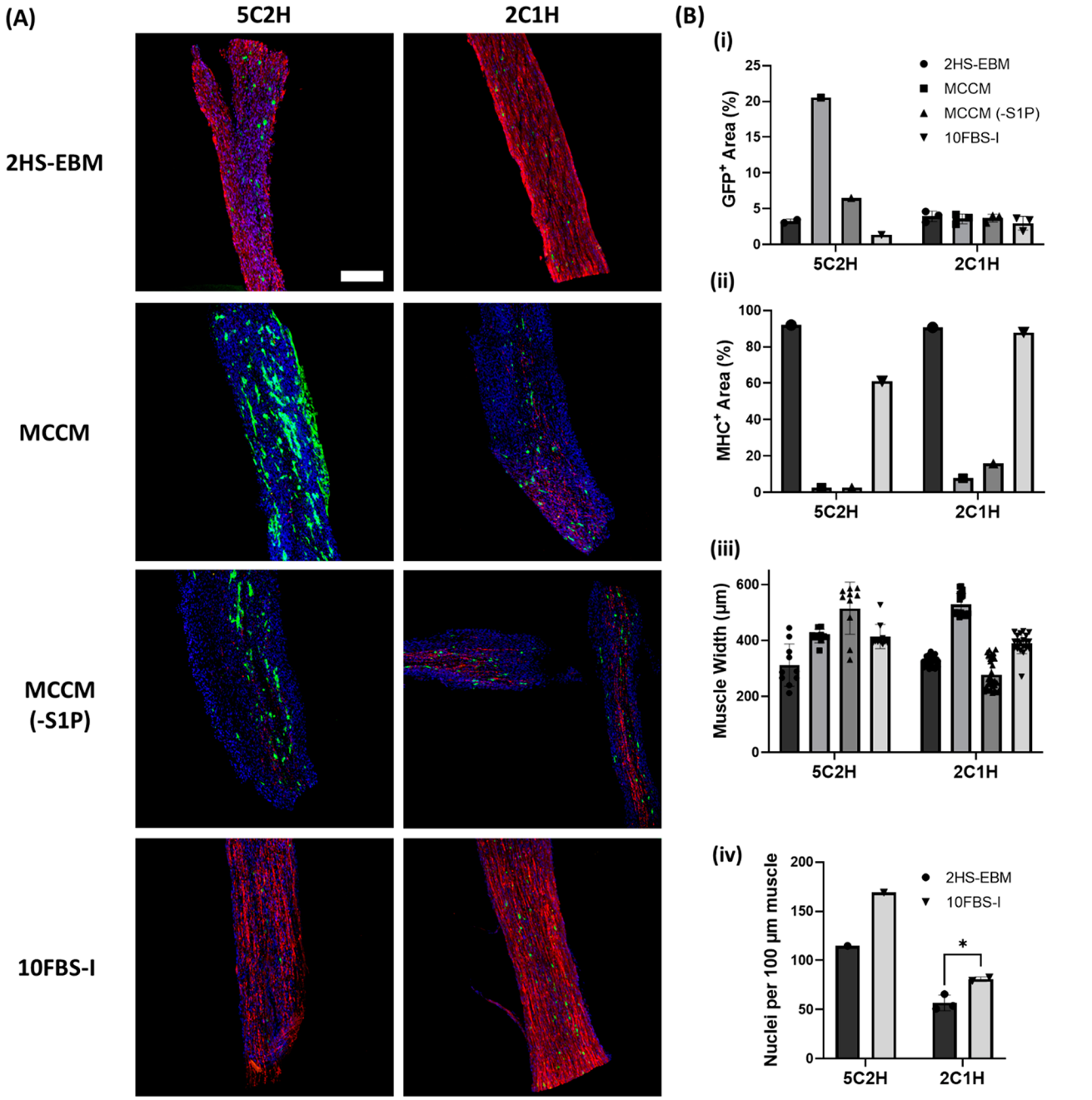

Figure 3. Myoblasts and endothelial cells cultured in 3D with different cell ratios and various culture media. (A) Fluorescently stained cryosections (30 μm thick) of muscle and endothelial cells cocultured in MF gels for 14 days in different culture media (Table 1). Media changes were performed every 2 days. MHC stained red, nuclei stained blue, and GFP-HUVECs stained green. 5CH2 represents 5 million C2C12s, 2 million HUVECs, and 500 000 10T1/2s/mL, and 2C1H represents 2 million C2C12s, 1 million HUVECs, and 250 000 10T1/2s/mL. Scale bar: 250 μm for all panels. (B) Various metrics were quantified from A. (i) Percent area of the tissue sections expressing GFP (from GFP-HUVECs). N = 2 for 2HS-EBM (5C2H) and N = 1 for MCCM, MCCM (-S1P), 10FBS-I (5C2H). N = 3 for all 2C1H samples. (ii) Percent area of the tissue sections positively stained for MHC. N = 1 for all samples. (iii) Measurements of the *in vitro* muscle construct width. Ten measurements per cryosection. N = 1 (# of cryosections measured) for 5C2H samples. For 2C1H samples, N = 2 for MCCM and 10FBS-I groups and N = 3 for MCCM (-S1P) and 2HS-EBM groups. (***) represents $p \leq 0.001$, and a full table of comparisons is available in Table S1. (iv) Number of nuclei present in 3D tissue engineered muscles per 100 μm of muscle length. N = 3 for 2HS-EBM, N = 2 for 10FBS-I, 2C1H cell seeding ratio. N = 1 for 5C2H groups. (*) represents $p \leq 0.05$ for an unpaired t test between 2HS-EBM and 10FBS-I in the 2C1H cell seeding group. Higher magnification images (including cross sections) of tissues grown in 10FBS-1 and 2HS-EBM are available in Figure S2, paired with graphs of myotube alignment data for those sample groups.

3D *in vitro* muscle tissue. Muscle fiber alignment was determined by inputting micrographs of MHC stained cryosections into ImageJ's "Analyze → Directionality" function, set to 90 bins with the Fourier Components method.[16] Prior to calculation in ImageJ, MHC stained micrographs were converted into binary images by using ilastik. ilastik was superior to conventional thresholding when segmenting individual myotubes for the alignment analysis.[20] To calculate "Nuclei per 100 μm of muscle" fluorescently stained nuclei in the cryosections were counted via ImageJ's "Find Maxima" function and normalized to every 100 μm of *in vitro* muscle tissue length.

https://doi.org/10.1021/acsbiomaterials.3c00358
ACS Biomater. Sci. Eng. 2023, 9, 4558−4566

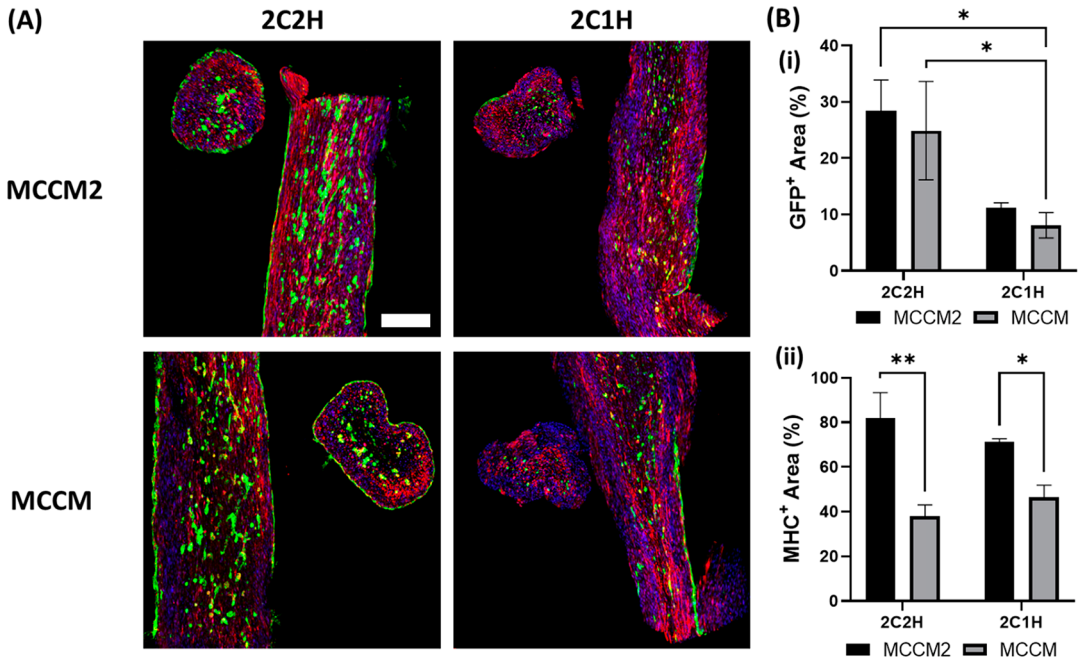

Figure 4. 3D muscle tissues containing endothelial cells, cultured in an updated coculture medium with a higher proportion of endothelial and endothelial-support cells. (A) Cryosections (30 μm) of muscle-endothelial tissues with either 2 million C2C12s, 2 million HUVECs, 500 000 10T1/2s/mL in the initial MF hydrogel (2C2H), or 2 million C2C12s, 1 million HUVECs, 250 000 10T1/2s/mL (2C1H). Tissues were cultured in either MCCM2 or MCCM (Table 1) for 14 days. Media changes were performed daily. Longitudinal and cross-sectional pieces of 3D muscle tissues were imaged together in the same frame. Red represents MHC, blue represents nuclei, and green represents GFP-HUVECs. Scale bar is 250 μm for all panels. (B) GFP and MHC quantified from A. (i) percent area of the tissue sections expressing GFP from HUVECs. (*) represents $p \leq 0.05$, all other comparisons were not significant. (ii) % area of the tissue sections positively staining for MHC. (*) represents $p \leq 0.05$, while (**) represents $p \leq 0.01$. $N = 3$ for 2C1H and MCCM samples and $N = 2$ for all other groups. Higher magnification micrographs of 2C2H/MCCM2 tissues are available in Figure S3, along with myotube alignment data.

Statistical Analyses. GraphPad Prism 9.3.1 and 9.4.1 were used for statistical analyses. For 2 sample groups, Student's t tests (unpaired, two-tailed) were performed. For 3 sample groups or more, analyses of variance (ANOVAs) were performed with Tukey's posthoc test for multiple comparisons. 0.05 was the cutoff P value for statistical significance, and error bars represent ±1 standard deviation.

RESULTS

Muscle Coculture Media enhances myogenic differentiation in 2D culture with C2C12 myoblasts. To coculture muscle and endothelial cells, MCCM was formulated with compounds reported to be beneficial to muscle differentiation and endothelial vessel formation (VEGF, dexamethasone, IGF-1, S1P).[21−25] C2C12s were differentiated in either MCCM or a more conventional 2% horse serum-based myogenic differentiation formulation (2HS-EBM) for 7 days (Figure 1A). MCCM resulted in a high degree of muscle differentiation from C2C12s with a fusion index of 0.818 (±0.159 SD), compared to 0.143 (±0.047 SD) with 2HS-EBM (Figure 1B).

Optimal Culture Media Formulations for C2C12s in 2D Do Not Necessarily Translate to 3D Culture. With the MCCM formulation, we next cultured C2C12s in 3D culture using MF gels based on a comparison between Matrigel-collagen and MF as tissue culture scaffolds where MF gels yielded the best performing 3D muscle constructs (according to *in vitro* muscle size and contractile force).[26] Unlike in 2D, 3D muscles grown in the MCCM did not generate a high degree of MHC expression (Figure 2A, i and ii). The MHC+ area of tissues cultured in 2HS-EBM was significantly higher than that of MCCM tissues (52.1% ± 9.2 SD versus 9.4% ± 4.1 SD, respectively; Figure 2B, i. MCCM may have had a proliferative rather than differentiating effect on the cultured cells, as we observed over 3 times more nuclei in MCCM treated tissues versus 2HS-EBM tissues (Figure 2B, ii). At the same time, MCCM treated tissues were observed to be larger than 2HS-EBM tissues (351.0 μm tissue width ±35.6 SD versus 173.2 μm ± 24.9 SD, respectively), possibly due to a combination of the higher cell numbers and decreased cell compaction (Figure 2B, iii). Myotubes cultured using 2HS-EBM and MCCM within the *in vitro* muscle bundles exhibited relatively uniform alignment along the axis of tension between the posts used to restrain the 3D tissues (Figure 2A, iii and iv; Figure S1).

Sphingosine-1-phosphate-containing Coculture Media Promotes Endothelial Cell Survival in *In Vitro* Muscle Constructs, while 10% FBS, Insulin, and IGF-1-containing Media Appear to Potently Support 3D Myogenesis. Due to the unexpected results with MCCM during 3D muscle tissue culture, both MCCM and 2HS-EBM were used when performing a larger screen of various culture media on the differentiation of *in vitro* muscle-endothelial tissues. MCCM without S1P was also tested to assess the potency of this ingredient in promoting endothelial cell growth and differentiation. Last, a new 10% FBS-based coculture media formulation (10FBS-I) was introduced. 10FBS-I includes 10 μg/mL insulin and 100 ng/mL IGF-1 as additional supplements intended to promote myogenesis. MF gels were seeded with reduced C2C12 concentrations to avoid overcrowding the endothelial cells during muscle-endothelial cocultures. 3D muscle tissues were seeded with 5

https://doi.org/10.1021/acsbiomaterials.3c00358
ACS Biomater. Sci. Eng. 2023, 9, 4558−4566

million C2C12s, 2 million HUVECs, and 500k 10T1/2s/mL (5C2H), or 2 million C2C12s, 1 million HUVECs, and 250k 10T1/2s/mL (2C1H). After 14 days of culture, 3D muscle-endothelial cocultures yielded polarizing results depending on the media formulation used (Figure 3A). Cells cultured in MCCM with the 5C2H cell seeding density contained more GFP (representing GFP-HUVECs) than other samples, at 20.55% (Figure 3B, i), although these results are based on limited replicates. Weaker GFP-HUVEC performance was observed in MCCM (-S1P) and other groups. The removal of S1P in MCCM (-S1P) did not appear to result in enhanced MHC expression (Figure 3B, ii).

For both 5C2H and 2C1H groups, 2.5% to 16% of sectioned *in vitro* muscle tissues stained positive for MHC when cultured in MCCM (and MCCM (-S1P)), while muscle tissues cultured in 2HS-EBM and 10FBS-I were 61% to 92% MHC positive based on our initial observations (Figure 3B, ii). In terms of tissue width, 10FBS-I treated tissues were generally observed to be wider than 2HS-EBM tissues (Figure 3B, iii). Concurrently, a higher number of nuclei were observed in 2C1H, 10FBS-I tissues when compared to 2C1H, 2HS-EBM groups (Figure 3B, iv).

Both Media and Cell Concentrations Need to Be Optimized to Produce Endothelialized *In Vitro* Muscle. *In vitro* muscles were cultured in MCCM2, a 1-to-1 ratio of MCCM and 10FBS-I (Figure 4A), and the result was improved muscle differentiation in muscle-endothelial cocultures. 10FBS-I was chosen to be paired with MCCM over 2HS-EBM because it appeared to promote both cell proliferation and myogenic differentiation to ultimately form larger tissues, while also achieving more uniform MHC expression through the entire thickness of the tissues, as observed in cross sections of our cell-cultured muscle tissues (Figure S2A). A new cell ratio (2C2H) was also tested, reflecting a combination of the 5C2H and 2C1H cell ratios from the previous experiment where more robust muscle development was observed in the 2 million C2C12s/mL (2C1H) group, while more endothelialization was observed in the 2 million HUVECs/mL (5C2H) group. Compared to MCCM, MCCM2 increased MHC expression in 2C1H cocultures from 46.38% (±0.06 SD) to 71.28% (±0.01 SD), while in 2C2H cocultures MHC increased from 38.01% (±0.05 SD) to 81.83% (±0.12 SD) (Figure 4B, ii). At the same time, MCCM2 did not adversely affect GFP-HUVEC performance, based on GFP expression, for both 2C2H and 2C1H groups (Figure 4B, i). Compared to 2C1H, an over 3-fold improvement in HUVEC GFP expression was observed in the 2C2H groups (Figure 4B, i)). For MHC expression, no significant differences were observed between 2C2H and 2C1H (Figure 4B, ii).

DISCUSSION

In this study, we combined cell types from different species (human endothelial cells with murine C2C12s and 10T1/2s) in a 3D coculture system to investigate the potential for vascularized *in vitro*-grown muscle tissue. These cell types were used as model cell lines for muscle and endothelial cells during the establishment of our 3D muscle-endothelial culture system. The rationale behind using these cell types is based on existing precedent in the literature, which has demonstrated the successful combination of C2C12s and HUVECs in muscle-endothelial cocultures.[13,27] The pairing of HUVECs with 10T1/2 cells is also commonly reported in the literature.[28−30] This project lays the groundwork for future investigations to confirm optimal conditions for cocultures of other cell type combinations, including human, livestock, or fish cell types. In the current system, our results suggest that when culturing muscle and endothelial cells to form a 3D endothelialized muscle construct *in vitro*, both culture media formulations and cell ratios need to be optimized in order to obtain tissues with both robust MHC^+ and GFP^+ phenotypes. Ultimately, a coculture media formulation (MCCM2) was developed here that allows for the simultaneous *in vitro* culture of muscle and endothelial cells.

During the testing of muscle-endothelial coculture media, one formulation (MCCM) differentiated C2C12s robustly in 2D, but not in 3D. It is unclear why this trend occurred, though one case of a growth factor (transforming growth factor beta 1, TGFβ1) having differential effects in 2D versus 3D culture has been reported in the past for skeletal muscle cells.[31] With this in mind, it is possible that the potentially anti-TGFβ1 effect of FGFβ (present in MCCM) could have played a role in the poorer outcomes with MCCM in 3D culture.[32] Differing optimal conditions for 2D and 3D culture have also been reported for fat cells, where stiff substrates inhibit adipogenesis during 2D culture but promote it during 3D culture.[33]

While myogenic differentiation was lacking with MCCM, endothelial cells in 3D tissues performed best with this formulation. This was only the case when MCCM was combined with a higher cell seeding density (5C2H). Improved outcomes from raising endothelial cell concentrations have been reported elsewhere for 3D muscle-endothelial cocultures, where increasing muscle and endothelial cell concentrations from 1 to 2 million cells/mL resulted in enhanced GFP expression (from GFP-HUVECs).[34] For muscle cells, a wide range of muscle cell concentrations (1 to >100 million cells/mL, see Table S2) have been used to successfully produce 3D muscles with robust myogenesis. Lower concentrations (such as the 1−2 million cells/mL used in this study) in particular have been used in other studies that investigated cocultures of muscle and endothelial cells.[15,34,35]

Regarding the formulation of MCCM, decreased GFP expression in the MCCM (-S1P) groups suggests that S1P promoted GFP-HUVEC performance in 3D muscle-endothelial tissues. S1P activates specific G-protein coupled receptors (GPCRs) expressed in endothelial cells and has been shown to enhance HUVEC DNA synthesis, migration, tube formation, and VEGF expression.[36−38] S1P removal did not influence MHC expression, which may suggest that S1P is a useful media additive that improves endothelial cell performance without impeding skeletal muscle differentiation. In other reports, S1P has been shown to enhance myogenesis and muscle differentiation.[39−44]

As MCCM promoted GFP-HUVEC activity while 10FBS-I promoted MHC+ muscle differentiation, we attempted to achieve simultaneous muscle differentiation and endothelialization by coculturing the two together in a 1-to-1 ratio of MCCM and 10FBS-I (i.e., MCCM2). 10FBS-I was chosen over 2HS-EBM (which also promoted myogenesis), as it resulted in the formation of larger muscle tissues. As 10% FBS is typically used to proliferate myoblasts *in vitro*, it is possible that 10FBS-I stimulated cell proliferation to result in larger 3D muscles. Indeed, 10FBS-I-cultured tissues contained significantly higher numbers of nuclei when compared with

https://doi.org/10.1021/acsbiomaterials.3c00358
ACS Biomater. Sci. Eng. 2023, 9, 4558−4566

2HS-EBM tissues. While muscle proliferation and differentiation are typically thought of as mutually exclusive events, other interventions that promote both processes exist, such as with the electrical stimulation of 3D cultured muscles.[45]

MCCM2 significantly enhanced MHC expression in 3D cultured muscles. Conversely, improved GFP expression was observed only with endothelial (and support) cells seeded at higher densities (2C2H vs 2C1H groups). This finding highlights the importance of optimizing both media formulation and cell seeding densities/ratios for the coculture of 3D muscle-endothelial tissues. Muscle-endothelial tissues cultured in MCCM2 with the 2C2H cell seeding concentration exhibited MHC expression across the full thickness of the tissue cross-section while promoting the highest HUVEC survival among the tested conditions.

A limitation of our study is the low number of replicates performed under some experimental conditions. Consequently, true optimal media compositions and cell ratios for fostering muscle differentiation and endothelial cell survival during 3D coculture may differ from what is reported in this study. However, overall trends observed here may hold true, such as how increased endothelial cell concentrations (e.g., from the 2C1H to the 2C2H cell ratio) in the cocultures improve 3D construct endothelialization. Despite these limitations, our study provides valuable preliminary insights on how cell ratios and media compositions can be optimized in tandem to potentially yield large boosts in muscle differentiation and endothelial cell survival within 3D muscle-endothelial tissues. In future investigations, we aim to increase the number of replicates and perform independent experiments to further validate and refine our findings as well as explore the possibility of incorporating biological replicates where feasible. A crucial aspect to address in subsequent steps is to assess whether the endothelial cells present in the muscle-endothelial constructs are able to form lumens, as their vessel function is hypothesized to be a key attribute in their ability to enable the survival of larger tissue engineered muscle constructs (by permitting the flow of culture media to the tissue interior). Future iterations of endothelialized muscles should include methods to improve vasculogenesis by the cocultured endothelial cells. For example, a further increase in endothelial cell concentration within muscle-endothelial tissues could have beneficial effects, as the initial increase from 1 to 2 million cells/mL significantly improved GFP-HUVEC performance. The ratio of endothelial cells to muscle and support cells can also be screened, as specific endothelial-support cell ratios have been reported to significantly improve capillary formation during *in vitro* hydrogel-based 3D cultures (e.g., a 7:1 endothelial to support cell ratio was reported to be optimal, while a 4:1 ratio was used in this study).[12] Other methods of cell seeding into or onto the 3D muscle constructs may also be beneficial, such as via a two-stage seeding process where a layer of endothelial cells are added as a coating on the outside of an *in vitro* 3D muscle piece.[15] Alternate endothelial cells to HUVECs may also be worth investigating such as MS1-VEGF cells. MS1-VEGFs have a high tolerance for varying culture media formulations (e.g., survival in high glucose media) that may also aid efforts to coculture muscle and endothelial cells, and the VEGF that they express may enhance myogenesis within *in vitro* muscle-endothelial constructs.[46−49] The validation of functional endothelial cell vascularization in 3D cultured muscles should be followed by the generation of larger tissues (>1 mm ⌀), such that the ability for a vessel network to truly permit the growth of larger cell-cultured muscle tissues can be assessed (Figure S4).

CONCLUSIONS

This work serves as the groundwork for achieving functionally vascularized *in vitro* 3D muscle tissue. We showcase *in vitro* muscle tissues (C2C12s) grown in 3D culture conditions with robust myosin expression that simultaneously supported the survival of endothelial cells (HUVECs). Cell culture experiments for these systems demonstrated that muscle cells in 2D and 3D may have different requirements while showing that culture media formula and cell ratios need to be simultaneously optimized to produce endothelialized muscle tissue *in vitro*. As 3D tissue culture continues to advance, its potential to produce *in vitro* muscles suitable for medical applications and sustainable food sources will grow, contributing to the ongoing transformation of the tissue engineering and biotechnology fields.

ASSOCIATED CONTENT

Supporting Information

The Supporting Information is available free of charge at https://pubs.acs.org/doi/10.1021/acsbiomaterials.3c00358.

(1) Additional experimental details: a photograph of the 3D muscle tissue culture's experimental set up; (2) additional statistical comparison data; (3) an overview of the 3D skeletal muscle tissue culture literature; (4) Higher magnification longitudinal and cross-sectional micrographs of stained in vitro muscle tissues from Figure 3; (5) Higher magnification longitudinal and cross-sectional micrographs of stained in vitro muscle tissues from Figure 4; (6) A fluorescently stained piece of macroscale sized *in vitro* 3D muscle (PDF)

AUTHOR INFORMATION

Corresponding Author

David L Kaplan − *David Kaplan Laboratory, Biomedical Engineering Department, Tufts University, Medford, Massachusetts 02215, United States;* orcid.org/0000-0002-9245-7774; Email: david.kaplan@tufts.edu

Authors

John SK Yuen Jr. − *David Kaplan Laboratory, Biomedical Engineering Department, Tufts University, Medford, Massachusetts 02215, United States*

Brigid M Barrick − *David Kaplan Laboratory, Biomedical Engineering Department, Tufts University, Medford, Massachusetts 02215, United States*

Hailey DiCindio − *David Kaplan Laboratory, Biomedical Engineering Department, Tufts University, Medford, Massachusetts 02215, United States*

Jaymie A Pietropinto − *David Kaplan Laboratory, Biomedical Engineering Department, Tufts University, Medford, Massachusetts 02215, United States*

Complete contact information is available at: https://pubs.acs.org/10.1021/acsbiomaterials.3c00358

Notes

The authors declare no competing financial interest.

■ ACKNOWLEDGMENTS

We thank ARPA-E (DE-AR0001233), the NIH (P41EB027062), New Harvest, and the United States Department of Defense (DoD) through the National Defense Science & Engineering Graduate (NDSEG) Fellowship Program.

■ REFERENCES

(1) Dessauge, F.; Schleder, C.; Perruchot, M.-H.; Rouger, K. 3D in Vitro Models of Skeletal Muscle: Myopshere, Myobundle and Bioprinted Muscle Construct. *Veterinary Research* **2021**, *52* (1), 72.
(2) Pollot, B. E.; Corona, B. T. Volumetric Muscle Loss. *Methods Mol. Biol.* **2016**, *1460*, 19−31.
(3) Nutter, G. P.; VanDusen, K. W.; Florida, S. E.; Syverud, B. C.; Larkin, L. M. The Effects of Engineered Skeletal Muscle on Volumetric Muscle Loss in the Tibialis Anterior of Rat After 3 Months In Vivo. *Regen. Eng. Transl. Med.* **2020**, *6*, 365.
(4) Helmlinger, G.; Yuan, F.; Dellian, M.; Jain, R. K. Interstitial PH and PO2 Gradients in Solid Tumors in Vivo: High-Resolution Measurements Reveal a Lack of Correlation. *Nature Medicine* **1997**, *3* (2), 177−182.
(5) Madden, L.; Juhas, M.; Kraus, W. E.; Truskey, G. A.; Bursac, N. Bioengineered Human Myobundles Mimic Clinical Responses of Skeletal Muscle to Drugs. *eLife* **2015**, *4*, No. e04885.
(6) Agrawal, G.; Aung, A.; Varghese, S. Skeletal Muscle-on-a-Chip: An in Vitro Model to Evaluate Tissue Formation and Injury. *Lab Chip* **2017**, *17* (20), 3447−3461.
(7) Prüller, J.; Mannhardt, I.; Eschenhagen, T.; Zammit, P. S.; Figeac, N. Satellite Cells Delivered in Their Niche Efficiently Generate Functional Myotubes in Three-Dimensional Cell Culture. *PLoS One* **2018**, *13* (9), No. e0202574.
(8) Khodabukus, A.; Kaza, A.; Wang, J.; Prabhu, N.; Goldstein, R.; Vaidya, V. S.; Bursac, N. Tissue-Engineered Human Myobundle System as a Platform for Evaluation of Skeletal Muscle Injury Biomarkers. *Toxicol. Sci.* **2020**, *176* (1), 124−136.
(9) Dennis, R. G.; Kosnik, P. E., II Excitability and Isometric Contractile Properties of Mammalian Skeletal Muscle Constructs Engineered in Vitro. *In Vitro Cell. Dev. Biol. Anim.* **2000**, *36* (5), 327−335.
(10) Cuchiara, M. P.; Gould, D. J.; McHale, M. K.; Dickinson, M. E.; West, J. L. Integration of Self-Assembled Microvascular Networks with Microfabricated PEG-Based Hydrogels. *Adv. Funct. Mater.* **2012**, *22* (21), 4511−4518.
(11) Li, Y.; Pi, Q.-M.; Wang, P.-C.; Liu, L.-J.; Han, Z.-G.; Shao, Y.; Zhai, Y.; Zuo, Z.-Y.; Gong, Z.-Y.; Yang, X.; Wu, Y. Functional Human 3D Microvascular Networks on a Chip to Study the Procoagulant Effects of Ambient Fine Particulate Matter. *RSC Adv.* **2017**, *7* (88), 56108−56116.
(12) Wan, Z.; Zhong, A. X.; Zhang, S.; Pavlou, G.; Coughlin, M. F.; Shelton, S. E.; Nguyen, H. T.; Lorch, J. H.; Barbie, D. A.; Kamm, R. D. A Robust Method for Perfusable Microvascular Network Formation In Vitro. *Small Methods* **2022**, *6* (6), 2200143.
(13) Koffler, J.; Kaufman-Francis, K.; Shandalov, Y.; Egozi, D.; Amiad Pavlov, D.; Landesberg, A.; Levenberg, S. Improved Vascular Organization Enhances Functional Integration of Engineered Skeletal Muscle Grafts. *Proc. Natl. Acad. Sci. U.S.A.* **2011**, *108* (36), 14789−14794.
(14) Perry, L.; Flugelman, M. Y.; Levenberg, S. Elderly Patient-Derived Endothelial Cells for Vascularization of Engineered Muscle. *Molecular Therapy* **2017**, *25* (4), 935−948.
(15) Gholobova, D.; Terrie, L.; Mackova, K.; Desender, L.; Carpentier, G.; Gerard, M.; Hympanova, L.; Deprest, J.; Thorrez, L. Functional Evaluation of Prevascularization in One-Stage versus Two-Stage Tissue Engineering Approach of Human Bio-Artificial Muscle. *Biofabrication* **2020**, *12* (3), 035021.
(16) Schneider, C. A.; Rasband, W. S.; Eliceiri, K. W. NIH Image to ImageJ: 25 Years of Image Analysis. *Nat. Methods* **2012**, *9* (7), 671−675.
(17) Maffioletti, S. M.; Sarcar, S.; Henderson, A. B. H.; Mannhardt, I.; Pinton, L.; Moyle, L. A.; Steele-Stallard, H.; Cappellari, O.; Wells, K. E.; Ferrari, G.; Mitchell, J. S.; Tyzack, G. E.; Kotiadis, V. N.; Khedr, M.; Ragazzi, M.; Wang, W.; Duchen, M. R.; Patani, R.; Zammit, P. S.; Wells, D. J.; Eschenhagen, T.; Tedesco, F. S. Three-Dimensional Human IPSC-Derived Artificial Skeletal Muscles Model Muscular Dystrophies and Enable Multilineage Tissue Engineering. *Cell Reports* **2018**, *23* (3), 899−908.
(18) Kemp, S. S.; Aguera, K. N.; Cha, B.; Davis, G. E. Defining Endothelial Cell-Derived Factors That Promote Pericyte Recruitment and Capillary Network Assembly. *ATVB* **2020**, *40*, 2632.
(19) Morin, K. T.; Dries-Devlin, J. L.; Tranquillo, R. T. Engineered Microvessels with Strong Alignment and High Lumen Density Via Cell-Induced Fibrin Gel Compaction and Interstitial Flow. *Tissue Eng. Part A* **2014**, *20* (3−4), 553−565.
(20) Berg, S.; Kutra, D.; Kroeger, T.; Straehle, C. N.; Kausler, B. X.; Haubold, C.; Schiegg, M.; Ales, J.; Beier, T.; Rudy, M.; Eren, K.; Cervantes, J. I.; Xu, B.; Beuttenmueller, F.; Wolny, A.; Zhang, C.; Koethe, U.; Hamprecht, F. A.; Kreshuk, A. Ilastik: Interactive Machine Learning for (Bio)Image Analysis. *Nat. Methods* **2019**, *16* (12), 1226−1232.
(21) Patil, S. D.; Papadmitrakopoulos, F.; Burgess, D. J. Concurrent Delivery of Dexamethasone and VEGF for Localized Inflammation Control and Angiogenesis. *J. Controlled Release* **2007**, *117* (1), 68−79.
(22) Lin, S.; Zhang, Q.; Shao, X.; Zhang, T.; Xue, C.; Shi, S.; Zhao, D.; Lin, Y. IGF-1 Promotes Angiogenesis in Endothelial Cells/Adipose-Derived Stem Cells Co-Culture System with Activation of PI3K/Akt Signal Pathway. *Cell Prolif* **2017**, *50* (6), e12390.
(23) Danieli-Betto, D.; Peron, S.; Germinario, E.; Zanin, M.; Sorci, G.; Franzoso, S.; Sandonà, D.; Betto, R. Sphingosine 1-Phosphate Signaling Is Involved in Skeletal Muscle Regeneration. *American Journal of Physiology-Cell Physiology* **2010**, *298* (3), C550−C558.
(24) Han, D.-S.; Yang, W.-S.; Kao, T.-W. Dexamethasone Treatment at the Myoblast Stage Enhanced C2C12 Myocyte Differentiation. *Int. J. Med. Sci.* **2017**, *14* (5), 434−443.
(25) Belair, D. G.; Whisler, J. A.; Valdez, J.; Velazquez, J.; Molenda, J. A.; Vickerman, V.; Lewis, R.; Daigh, C.; Hansen, T. D.; Mann, D. A.; Thomson, J. A.; Griffith, L. G.; Kamm, R. D.; Schwartz, M. P.; Murphy, W. L. Human Vascular Tissue Models Formed from Human Induced Pluripotent Stem Cell Derived Endothelial Cells. *Stem Cell Rev.* **2015**, *11* (3), 511−525.
(26) Hinds, S.; Bian, W.; Dennis, R. G.; Bursac, N. The Role of Extracellular Matrix Composition in Structure and Function of Bioengineered Skeletal Muscle. *Biomaterials* **2011**, *32* (14), 3575−3583.
(27) Yeo, M.; Kim, G. Micro/Nano-Hierarchical Scaffold Fabricated Using a Cell Electrospinning/3D Printing Process for Co-Culturing Myoblasts and HUVECs to Induce Myoblast Alignment and Differentiation. *Acta Biomaterialia* **2020**, *107*, 102−114.
(28) Koike, N.; Fukumura, D.; Gralla, O.; Au, P.; Schechner, J. S.; Jain, R. K. Creation of Long-Lasting Blood Vessels. *Nature* **2004**, *428* (6979), 138−139.
(29) Moon, J. J.; Saik, J. E.; Poché, R. A.; Leslie-Barbick, J. E.; Lee, S.-H.; Smith, A. A.; Dickinson, M. E.; West, J. L. Biomimetic Hydrogels with Pro-Angiogenic Properties. *Biomaterials* **2010**, *31* (14), 3840−3847.
(30) Zhu, W.; Qu, X.; Zhu, J.; Ma, X.; Patel, S.; Liu, J.; Wang, P.; Lai, C. S. E.; Gou, M.; Xu, Y.; Zhang, K.; Chen, S. Direct 3D Bioprinting of Prevascularized Tissue Constructs with Complex Microarchitecture. *Biomaterials* **2017**, *124*, 106−115.
(31) Krieger, J.; Park, B.-W.; Lambert, C. R.; Malcuit, C. 3D Skeletal Muscle Fascicle Engineering Is Improved with TGF-B1 Treatment of Myogenic Cells and Their Co-Culture with Myofibroblasts. *PeerJ.* **2018**, *6*, No. e4939.
(32) Kawai-Kowase, K.; Sato, H.; Oyama, Y.; Kanai, H.; Sato, M.; Doi, H.; Kurabayashi, M. Basic Fibroblast Growth Factor Antagonizes Transforming Growth Factor-B1-Induced Smooth Muscle Gene Expression Through Extracellular Signal-Regulated

https://doi.org/10.1021/acsbiomaterials.3c00358
ACS Biomater. Sci. Eng. 2023, 9, 4558−4566

Kinase 1/2 Signaling Pathway Activation. *Arterioscler., Thromb., Vasc. Biol.* **2004**, *24* (8), 1384−1390.
(33) Oliver-De La Cruz, J.; Nardone, G.; Vrbsky, J.; Pompeiano, A.; Perestrelo, A. R.; Capradossi, F.; Melajová, K.; Filipensky, P.; Forte, G. Substrate Mechanics Controls Adipogenesis through YAP Phosphorylation by Dictating Cell Spreading. *Biomaterials* **2019**, *205*, 64−80.
(34) Gholobova, D.; Decroix, L.; Van Muylder, V.; Desender, L.; Gerard, M.; Carpentier, G.; Vandenburgh, H.; Thorrez, L. Endothelial Network Formation Within Human Tissue-Engineered Skeletal Muscle. *Tissue Eng. Part A* **2015**, *21* (19−20), 2548−2558.
(35) Thorrez, L.; DiSano, K.; Shansky, J.; Vandenburgh, H. Engineering of Human Skeletal Muscle With an Autologous Deposited Extracellular Matrix. *Front. Physiol.* **2018**, *9*, DOI: 10.3389/fphys.2018.01076.
(36) Lee, O.-H.; Kim, Y.-M.; Lee, Y. M.; Moon, E.-J.; Lee, D.-J.; Kim, J.-H.; Kim, K.-W.; Kwon, Y.-G. Sphingosine 1-Phosphate Induces Angiogenesis: Its Angiogenic Action and Signaling Mechanism in Human Umbilical Vein Endothelial Cells. *Biochem. Biophys. Res. Commun.* **1999**, *264* (3), 743−750.
(37) Mendelson, K.; Evans, T.; Hla, T. Sphingosine 1-Phosphate Signalling. *Development* **2014**, *141* (1), 5−9.
(38) Heo, K.; Park, K.-A.; Kim, Y.-H.; Kim, S.; Oh, Y.-S.; Kim, I.-H.; Ryu, S.; Suh, P.-G. Sphingosine 1-Phosphate Induces Vascular Endothelial Growth Factor Expression in Endothelial Cells. *BMB reports* **2009**, *42*, 685−690.
(39) Bernacchioni, C.; Cencetti, F.; Blescia, S.; Donati, C.; Bruni, P. Sphingosine Kinase/Sphingosine 1-Phosphate Axis: A New Player for Insulin-like Growth Factor-1-Induced Myoblast Differentiation. *Skeletal Muscle* **2012**, *2* (1), 15.
(40) Ieronimakis, N.; Pantoja, M.; Hays, A. L.; Dosey, T. L.; Qi, J.; Fischer, K. A.; Hoofnagle, A. N.; Sadilek, M.; Chamberlain, J. S.; Ruohola-Baker, H.; Reyes, M. Increased Sphingosine-1-Phosphate Improves Muscle Regeneration in Acutely Injured Mdx Mice. *Skeletal Muscle* **2013**, *3* (1), 20.
(41) Loh, K. C.; Leong, W.-I.; Carlson, M. E.; Oskouian, B.; Kumar, A.; Fyrst, H.; Zhang, M.; Proia, R. L.; Hoffman, E. P.; Saba, J. D. Sphingosine-1-Phosphate Enhances Satellite Cell Activation in Dystrophic Muscles through a S1PR2/STAT3 Signaling Pathway. *PLoS One* **2012**, *7* (5), No. e37218.
(42) Donati, C.; Meacci, E.; Nuti, F.; Becciolini, L.; Farnararo, M.; Bruni, P. Sphingosine 1-Phosphate Regulates Myogenic Differentiation: A Major Role for S1P2 Receptor. *FASEB J.* **2005**, *19* (3), 1−22.
(43) Fortier, M.; Figeac, N.; White, R. B.; Knopp, P.; Zammit, P. S. Sphingosine-1-Phosphate Receptor 3 Influences Cell Cycle Progression in Muscle Satellite Cells. *Dev. Biol.* **2013**, *382* (2), 504−516.
(44) Squecco, R.; Sassoli, C.; Nuti, F.; Martinesi, M.; Chellini, F.; Nosi, D.; Zecchi-Orlandini, S.; Francini, F.; Formigli, L.; Meacci, E. Sphingosine 1-Phosphate Induces Myoblast Differentiation through Cx43 Protein Expression: A Role for a Gap Junction-Dependent and -Independent Function. *MBoC* **2006**, *17* (11), 4896−4910.
(45) Khodabukus, A.; Madden, L.; Prabhu, N. K.; Koves, T. R.; Jackman, C. P.; Muoio, D. M.; Bursac, N. Electrical Stimulation Increases Hypertrophy and Metabolic Flux in Tissue-Engineered Human Skeletal Muscle. *Biomaterials* **2019**, *198*, 259−269.
(46) Liu, J.; Hao, H.; Xia, L.; Ti, D.; Huang, H.; Dong, L.; Tong, C.; Hou, Q.; Zhao, Y.; Liu, H.; Fu, X.; Han, W. Hypoxia Pretreatment of Bone Marrow Mesenchymal Stem Cells Facilitates Angiogenesis by Improving the Function of Endothelial Cells in Diabetic Rats with Lower Ischemia. *PLoS One* **2015**, *10* (5), No. e0126715.
(47) Zou, W.; Liu, B.; Wang, Y.; Shi, F.; Pang, S. Metformin Attenuates High Glucose-Induced Injury in Islet Microvascular Endothelial Cells. *Bioengineered* **2022**, *13* (2), 4385−4396.
(48) Huey, K. A. Potential Roles of Vascular Endothelial Growth Factor During Skeletal Muscle Hypertrophy. *Exercise and Sport Sciences Reviews* **2018**, *46* (3), 195−202.
(49) Liu, M.; Zhang, X.; Wang, B.; Wu, Q.; Li, B.; Li, A.; Zhang, H.; Xiu, R. Functional Status of Microvascular Vasomotion Is Impaired in Spontaneously Hypertensive Rat. *Sci. Rep.* **2017**, *7*, 178080.

https://doi.org/10.1021/acsbiomaterials.3c00358
ACS Biomater. Sci. Eng. 2023, 9, 4558−4566